

Hybrid Multi-Channel EEG Filtering Method for Ocular and Muscular Artifact Removal Based on the 3D Spline Interpolation Technique

AFEF ABIDI^{1,2}, IBTIHEL NOUIRA^{1,*}, INES ASSALI¹, MOHAMED ALI SAAFI¹
AND MOHAMED HEDI BEDOUI¹

¹Technology and Medical Imaging Laboratory, Faculty of Medicine Monastir, University of Monastir,
Monastir 5019, Tunisia

²National Engineering School of Sousse, University of Sousse, BP 264 Erriyadh, Sousse 4023, Tunisia

*Corresponding author: ibtihelnouira@gmail.com

The present work develops a novel hybrid method for ocular and muscular artifact removal from electroencephalography (EEG) signals, EFICA-TQWT. It is a combination of efficient fast independent component analysis (EFICA) method with the tunable Q-factor wavelet transform (TQWT). The main contribution of this paper is to apply the 3D interpolation method in the filtering system. Three EEG datasets are used in this work, two healthy and one epileptic. The choice of subjects for each dataset is made with the help of an expert in physiology. The selection criterion adopted is the presence of muscular and ocular artifacts in the processed recordings. First, a noisy channel automatic classification is performed by the support vector machine (SVM) with radial basis function in order to delete the signal(s) corresponding to the noisiest channel(s) from each EEG recording. The results of the automatic classification by the SVM were compared with those found by the expert's classification. An accuracy of 97.45%, a sensitivity of 86.66% and a 100% specificity are provided by the SVM classification. The hybrid method of artifact removal will be applied on the rest of the EEG channels of international 10/20 system for each subject. Then, a reconstruction of the eliminated channel signal(s) will be performed in order to obtain a well-filtered signal. The proposed filtering process is evaluated by calculating the mean squared error (MSE) and the signal to noise ratio (SNR). Both for the healthy and pathological EEG datasets, a comparative study of the proposed method (EFICA-TQWT) and other filtering techniques (Fast-ICA, DWT, TQWT and EFICA) is generated. The EFICA-TQWT method gave the best results with a minimum of MSE and a maximum of SNR, more particularly in the case of the application of the 3D interpolation method. Besides, in order to optimize the computing time of the proposed system, a parallel implementation of this filtering system is developed based on graphical processing units using compute unified device architecture.

Keywords: ocular and muscular artifact; hybrid method; efficient fast independent component; tunable Q-factor wavelet transform; support vector machine; evaluation criteria; graphical processing units

Received 19 March 2020; Revised 6 November 2020; Editorial Decision 8 November 2020

Handling editor: Dr Dimitrios Tzovaras

1. INTRODUCTION

The electroencephalography (EEG) involves measuring the electrical activity of the brain using electrodes placed on the surface of the scalp. The number and configuration of these

electrodes have a significant influence on all recording results. The use of a single electrode allows the recording of a small part of the cortical activity, whereas the simultaneous recording of many channels provides an overall representation of the neuronal electrical activity. These EEG recordings are mainly

used by the neurologist for detection of some grapho-elements (slow waves and spikes) and for diagnosis of tumors, epilepsy and other medical conditions [1, 2].

Recently, the EEG has played a great role in brain computer interface (BCI) applications [3]. Unfortunately, these EEG signals can be heavily contaminated by spurious signals called artifacts, which have their main origins in ocular activity, muscle activity, heart rate and slight electrode movements [4, 5]. In fact, the two physiological artifacts that are most problematic for BCI applications are the ocular (OA) and muscular artifacts (MA) [6]. Ocular artifacts are either generated by the eye rolling or eye blinks that occur ~ 20 times per minute [7]. This type of artifacts is located mostly in the anterior head regions with a maximal frequency range below 4 Hz. However, the muscular artifacts are characterized by a high-frequency range superior to 20 Hz with amplitudes varying from small to very large [8].

The presence of these artifacts hides the real forms of EEG signals. This results in misdiagnosis with a great risk of defective drugs or inadequate therapeutic protocols [9].

In order to have a real and clear image of brain activities and to facilitate the analysis of this type of signals, the artifact removal methods will be an urgent necessity in order to overcome the traditional EEG examination difficulties. These methods, which rely on the separation of sources, allow the determination of a set of cerebral origin sources and a set of artifact sources. The artifact sources are removed and the brain sources are used to reconstruct the signal.

In this context, many works have been conducted. More particularly, several studies have been interested in removing the ocular and muscular artifacts. For example, in [10] the authors proposed an artificial neural network (ANN) method to classify the artifactual and non-artifactual EEG dataset. Furthermore, they developed a novel time-amplitude algorithm for detecting the presence of eye movement artifact and multiple contaminated zones. Other works for artifact removal were performed based on blind source separation (BSS) [11] and including the older different versions of independent component analysis (ICA) algorithms [12, 13]. In fact, contrary to the regression methods, artifact removal methods based on ICA algorithm can conserve data on all scalp channels including frontal and particular locations [14]. As an example of artifact removal by ICA techniques, the work of [11] proposed to utilize the algorithm for multiple unknown source extraction and ICA–Infomax methods in order to isolate artifacts from 3-second EEG epochs.

Another artifact removal method based on stationary wavelet transform (SWT) was proposed to remove ocular artifacts from EEG signals [15, 16]. In these works, the SWT coefficients that correspond to the lower frequency ranges undergo a process of thresholding. Furthermore, the works of [17] proposed a hybrid brain-computer interface system based on the SWT combined with a novel adaptive thresholding mechanism to remove ocular and muscular artifacts. The proposed BCI system was composed of four main stages: artifact detection, artifact removal,

feature extraction module and feature classification. The filtering signals are obtained by applying an inverse SWT on the thresholded SWT coefficients. Some alternative studies aimed at eliminating EEG artifacts were performed. They were based on the hybrid WICA (wavelet-ICA) method [18]. Therefore, to improve the feature extraction performance of the EEG signals, the proposed approach includes the properties of three techniques: adaptive filtering, wavelet transform and ICA methods. The authors in [19] present numerical variable forgetting factor–recursive least squares method based on adaptive filtering in order to remove the ocular artifacts from the EEG signal. This method treats the separately recorded reference horizontal electro-oculogram (HEOG) and vertical electro-oculogram (VEOG) signals using finite impulse response filtering. Thereafter, the two HEOG and VEOG signals are removed from the recorded EEG signal to obtain a non-artifact EEG signal.

The main objective of this research work is to develop a new efficient method of EEG artifact removal. The first contribution in this paper is to use the efficient fast independent component analysis (EFICA) method, which is an advanced version of fast-ICA algorithm in order to remove ocular and muscular artifacts from EEG signals. In fact, apart from the medical domain, the EFICA is a technique used in several other fields such as speech feature extraction [20]. In order to further improve the filtering process efficiency of this algorithm, this work proposes to combine the EFICA technique with tunable Q-factor wavelet transform (TQWT). However, the filtering of very noisy signals is still a big problem in the field of signal processing. Indeed, even the most reliable filtering methods remain unable to give effective results for this type of signals. Accordingly, the major contribution in this paper focuses on the use of the 3D interpolation method [21] to filter the EEG signals of a large amount of artifacts. The proposed system extracts the noisiest electrode signal(s) by using the radial basis function (RBF) kernel based on the support vector machine (SVM). This (these) electrode(s) will be removed to filter the remaining less noisy channels of the EEG signals with the hybrid method, EFICA–TQWT. After that, a construction of the eliminated signal(s) will be carried out using the other filtered channels of the EEG signals. The evaluation of the novel hybrid method with and without interpolation is achieved by applying the evaluation criteria: mean squared error (MSE) and signal to noise ratio (SNR). Besides, an acceleration of the proposed filtering system based on graphical processing units (GPU) is given in order to meet the real-time processing requirement.

This paper is organized as follows: the dataset used is discussed in Section 2. The proposed method is described in Section 3. In Section 4, the obtained results are presented and discussed. Finally, the conclusion is covered in the last section.

2. MATERIALS

The effectiveness of the proposed EEG filtering system was evaluated in three different EEG datasets. The first one (dataset

1) corresponds to three healthy subjects, two males and one female aged from 20 to 30 years old. This EEG dataset was recorded by 19 electrodes according to the standard 10/20 system with a sampling frequency of 256 Hz and was provided by Sahloul Hospital, Sousse-Tunisia. Sixty-second long EEG records were taken with muscular and ocular artifacts.

The second one (dataset 2) of six pathological subjects (two males, four females) is provided by the Karunya University, India. This dataset was recorded by an 18-channel international 10/20 system, in which 16 electrodes are dedicated to scalp channels and the two other electrodes are pericardial channels with the references to left and right mastoids. The sampling frequency is 256 Hz and a data preprocessing has been applied with an analog pass-band filter of 0.01_100 Hz. Each recording was 10 s long, which is characterized by generalized and localized waves [22].

The third one (dataset 3) is related to 23 healthy recordings corresponding to 12 males and 11 females with an age range of 32 to 65 years. Each signal in this internationally recognized EEG dataset is characterized by its well-defined recording protocol and the details corresponding to subject (age, sex and the EEG waveforms), which are described in a given file. The EEG recordings were obtained using a 19-channel EEG digital video system with a sampling frequency of 250 Hz. The recording of each processed signal is 1 minute long.

All records from the three datasets are chosen with the help of an expert in physiology. These records are characterized by the presence of ocular and muscular artifacts, which can be observed on one or more channels. The approach proposed in this paper considers the raw data of the three datasets as inputs to the filtering system without any preprocessing process.

3. METHODS

The proposed filtering method is composed of four stages. The first one consists in classifying the noisiest EEG channel(s) from EEG recordings by applying the RBF kernel-based SVM. The second step is to eliminate the noisiest channel(s) and apply the hybrid EFICA-TQWT method on the rest EEG channels for ocular and muscular artifact removal. A reconstitution of the eliminated EEG signal(s) by applying the 3D spline method on the other filtered recordings will be carried out in the third step. The last stage permits to evaluate the EFICA-TQWT method with interpolation by calculating the MSE and SNR (Fig. 1).

3.1. Step 1: SVM

Thanks to its efficient generalization performance for the data of large dimension by dint of its convex optimization problem [23], different versions of SVM are widely used for classification in the biomedical field. For example, the work of [24, 25] exploited the generalized eigenvalue proximal carrier vector machine (GEPSVM) to detect pathological brain images from normal ones by using the MRI scanning. Similarly, Wang et

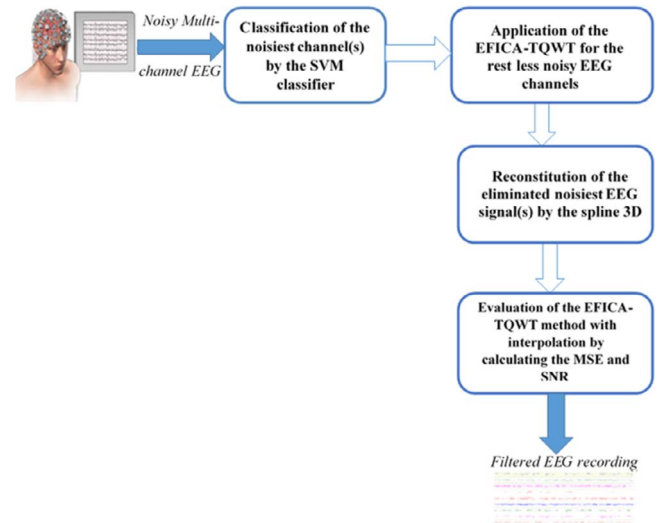


FIGURE 1. The multi-channel EEG analytical system block diagram for artifact removal.

al. [26] compared the efficiency of SVM, GEPSVM and twin SVM for the classification of MRI brain images. In addition, several works used multiple versions of SVM to classify the EEG signals according to epilepsy, movement, etc. [27–30]. The results showed that the RBF kernel SVM classifier offered better performance at the classification level [29–30]. Based on these results, this paper implements an RBF kernel SVM classifier to select the noisiest channel(s) by providing high accuracy and low algorithmic complexity.

To better justify the choice of the RBF kernel SVM and in addition to the accreditation on these different works [29–30], an empirical study was carried out by varying the kernels of the SVM algorithm. This study allows to know which kernel function best suits the classification problem in order to extract the noisiest channel(s) from all the used channels. For this study, three functions were considered: the linear, polynomial and RBF [31].

3.1.1. Theoretical SVM study

The SVM is a computational learning theory based on the classification and recognition method. Thanks to its ability to treat numerous predictors, the SVM is often used in biomedical classification applications [32].

For a classification problem of two linearly separable classes, the basis of SVM is to find a hyperplane H_0 that allows the separation of the entrance space with a maximum margin [32].

Let $X = \{x_1, \dots, x_l\}$, $x_i \in R^n$ a whole of training data vectors, $Y = \{y_1, \dots, y_l\}$, $y_i \in \{1, -1\}$ a corresponding labels set, w a normal weight vector to the hyperplane and b a bias, such that $b \in \mathcal{R}$.

To be adequately classified, the x_i and y_i vectors must verify Eq. 1 and Eq. 2 [33]:

$$wx_i + b \geq +1 \text{ for } y_i = +1 \quad (1)$$

$$wx_i + b \leq -1 \text{ for } y_i = -1 \quad (2)$$

In other words (Eq.3):

$$y_i (wx_i + b) \geq 1, \forall i \quad (3)$$

In fact, the performance of a linear SVM relies on a penalty parameter C, which equilibrates the relative importance corresponding to minimizing the learning error and maximizing class margins [30]. In the case of great C values, the optimization chooses a smaller margin hyperplane if the hyperplane correctly classifies the training points. However, for small values of parameter C, a larger margin hyperplane will be chosen even if more points are misclassified. Indeed, the SVM is transformed into a non-linear method in case a kernel trick technique is used. In that event, the hyperplane will be constructed in a higher-dimensional space, which is the transformation of low-dimensional input space by the kernel function [29]. Among the kernel functions, different works used the RBF kernel-based SVM for EEG classification [29–30]. This RBF kernel is optimized for two kernel parameters: the penalty factor C and the gamma parameter that specifies the similarity between points [30].

In fact, the RBF is characterized by the problem decision function, which is defined by Eq. 4 [31]:

$$F(x) = \text{sign} \left(\sum_{i=1}^n y_i \alpha_i k(x, x_i) + b \right) \quad (4)$$

with the $\alpha_i \geq 0$ are the Lagrange multipliers associated with the constraints and k is the kernel.

In the case of the RBF, the kernel is mathematically defined by Eq. 5 [34]:

$$k(x_i, x) = \exp(-\gamma \|x_i - x\|^2), \gamma > 0 \quad (5)$$

where $k(x_i, x)$ is the kernel function that is based on the inner-product of the two variants x_i and x ; and γ defines the scope of the influence of a single learning example.

To present the linear and polynomial function respectively, the kernel will be defined by Eq. 6 and Eq. 7:

$$K(x, x_i) = x \cdot x_i \quad (6)$$

$$K(x, x_i) = (1 + x \cdot x_i)^d, \quad (7)$$

where d is the polynomial degree, $d \geq 1$.

TABLE 1. Distribution of the EEG channel recordings into the training and testing sets.

Dataset	Total channels	Channels of the training phase	Channels of the test phase
Dataset 1	57	34	23
Dataset 2	96	58	38
Dataset 3	437	262	175
Total	590	354	236

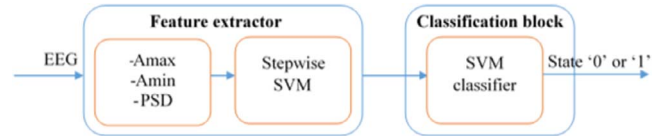


FIGURE 2. SVM blocks.

3.1.2. RBF kernel SVM classifier

All channels of different subjects for each dataset are used in the SVM classification system by dividing them into two parts. The first part, which includes 60% of the channels, is the training phase. The second part is the testing stage and it the rest of channels (40%) (Table 1). This division is chosen to balance the presence of the various ocular and muscular artifacts in the different EEG recordings by taking into account the inter-EEG channel division. In fact, the EEG channel recordings used to construct the training set are different from those used to evaluate the testing phase.

Indeed, the SVM classification is based on feature vector characterized every EEG signal of each channel. This vector is composed of three parameters. The first two parameters are taken from the temporal EEG signal, which are the EEG minimum and maximum amplitudes (Amin, Amax). The FFT was used to extract the third parameter in the frequency domain, which is the power spectral density.

The input data produced for the SVM are exposed in the form of an $N \times M$ matrix, where the rows and columns represent respectively the EEG channel signals and the extracted features. In fact, each EEG signal of the healthy subjects from dataset 1 (3) and dataset 3 (23) was recorded on 19 electrodes. However, the EEG recording corresponding to each epileptic patient (6) is represented on 16 channels. The total number of matrix rows is equal to 590 channels. $M + 1$ -column values are considered in order to distinguish the noisiest channels from the less noisy ones. In this work, a matrix of 590×4 was obtained. The stepwise SVM selects the features that best discriminate between the two output classes.

In this paper, for each subject, one or more channels are classified as the noisiest outputs. During testing, the SVM classifies EEG features as a state '0' (less noisy channel) or a state '1' (noisiest channel) (Fig. 2).

3.2. Step 2: ocular and muscular removal methods

The present work explores an evaluation study of proposed new ocular and muscular removal method of EEG signals. This method is the EFICA-TQWT, which is a hybrid method of EFICA algorithm of ICA with the TQWT.

In fact, the combination of these two techniques (EFICA with TQWT) was opted for because the ICA versions filter only the artifacts with the same or greater amplitudes than the useful EEG signal (muscular artifacts). However, the TQWT are effective just in the filtering of low frequencies (ocular artifacts) [9].

3.2.1. Theoretical study of filtering methods

• EFICA algorithm

In this paper, the efficient variant of fast-ICA (EFICA) algorithm was used. This method was proposed in [35]. It is based on the theory of fast-ICA, which is an advanced version of ICA algorithm. In fact, the objective of the ICA method is to find a data linear transformation. The ICA model is given by Eq. 8 [36]:

$$X = AS + v \quad (8)$$

with:

- X is a $d \times N$ matrix of unknown source signals, where x_{kl} is the (k, l) – th element. In this case, d is the mixed signal number and N is the sample number,
- S is the independent component (IC) source signals,
- A is the $d \times d$ unknown mixing matrix,
- v is the additive noise.

To rebuild the exact vector S , the v value is considered as zero. So, the ICA model is expressed as follows (Eq.9) [36]:

$$X = AS \quad (9)$$

The basic idea is to find the most characteristic direction in the feature space to make the signal independent of each other. Its main task is to find the inverse matrix with (Eq. 10, 11):

$$W = A^{-1} \quad (10)$$

So

$$S = WX \quad (11)$$

The emergence towards the fast-ICA allows to demix a set of statistically independent sources that have been mixed linearly. Traditional fast-ICA is the use of negative entropy to determine the non-Gaussian independent component [37]. This method determines the proximity of the independent component and can solve some real-time high-dimensional problems.

Note that $c(w_k)$ is an iterative optimization process (Eq. 12):

$$c(w_k) = E \left[G \left(w_k^T z \right) \right] \quad (12)$$

where:

- E stands for the sample mean,
- w_k^T is a row vector corresponding to the i^{th} source signal in the matrix W after k iterations,
- $G(\cdot)$ is a suitable nonlinear function, called contrast function (Eq. 13):

$$g = \frac{1}{\alpha_1} \log \cosh(\alpha_1 y), \quad (13)$$

— z is the inverse of the source signal X .

The symmetrical version of Fast-ICA estimates all original signals in parallel way. Each stage is finished by a symmetric orthogonalization (Eq.14) [35]:

$$w_k^+ = E \left[zg \left(w_k^+ z \right) \right] - w_k E \left[g' \left(w_k^+ z \right) \right] \quad (14)$$

where $g(\cdot)$ and $g'(i)$ indicate respectively the first and the second derivative of function $G(\cdot)$.

The EFICA algorithm, which is the improved version of fast-ICA, has three main steps [35]:

(A) Application of fast-ICA transformation of the source signal.

(B) A straightforward solution would be to choose $g_k(\cdot)$ as a score function that belongs to the sample distribution function.

For each $k = 1, \dots, d$; the adaptive choice of the nonlinear function $g \text{def} g_k$ is the approximation score function for the k^{th} component;

(C) Using Eq. 14 for iteration of $k = 1, \dots, d$; the corresponding final weight is (Eq. 15):

$$c_{kl} = \frac{V_{kl}^{1U}}{V_{lk}^{1U} + 1}, k \neq l; c_{kk} = 1; l = 1, \dots, d \quad (15)$$

where V_{kl}^{1U} is the Gaussian distribution variance of the normalized gain matrix elements $N^{1/2} G_{kl}^{1U}$. The G_{kl}^{1U} gain is obtained by the one-unit variant using a nonlinear function $g(\cdot)$ for the EFICA method [35].

So, the W_k^+ matrix; for each $k = 1, \dots, d$; is defined by Eq. 16:

$$W_k^+ = \left(\frac{c_{kl} w_l^+}{\|w_l^+\|}, \dots, \frac{c_{kd} w_d^+}{\|w_d^+\|} \right)^t \quad (16)$$

Thus, the symmetric orthogonal matrix W_k^+ obtains the final w_k estimate.

• Tunable Q-factor wavelet transform

The TQWT is used for signal decomposition, more particularly in biomedical signal analysis applications [38].

The TQWT is an advanced version of the wavelet transforms [39]. It has been recently developed to be dedicated to discrete-time signals. It is characterized by a Q -factor that is readily and continuously adjustable. This transformation is based on

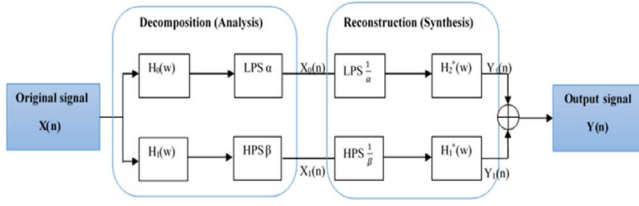


FIGURE 3. Analysis and synthesis filter banks of the TQWT.

the use of a bank of reversible oversampled filters with real-valued sampling factors. These filters are specified directly in the frequency domain (Fig. 3) [40].

In fact, the Q -factor is defined as the ratio between the center frequency f_0 and the bandwidth bw of the band pass filter (Eq. 17) [40]:

$$Q = \frac{f_0}{bw} \quad (17)$$

The TQWT is implemented using the concept of two-channel filter banks iteratively.

Noting α and β respectively the low-pass and high-pass scale factors for the two-channel filter bank, the frequency response of low-pass filter H_0 mathematically expressed as (Eq. 18) [41]:

$$H_0(w) = \begin{cases} 1, & |w| \leq (1 - \beta)\pi, \\ \theta\left(\frac{w + (\beta - 1)\pi}{\alpha + \beta - 1}\right), & (1 - \beta)\pi \leq |w| < \alpha\pi, \\ 0, & \alpha\pi \leq |w| \leq \pi, \end{cases} \quad (18)$$

The frequency response of high-pass filter can mathematically be expressed as Eq. 19 [41]:

$$H_1(w) = \begin{cases} 0, & |w| \leq (1 - \beta)\pi, \\ \theta\left(\frac{\alpha w - w}{\alpha + \beta - 1}\right), & (1 - \beta)\pi \leq |w| < \alpha\pi, \\ 1, & \alpha\pi \leq |w| \leq \pi, \end{cases} \quad (19)$$

where $\theta(\omega)$ is the Daubechies filter frequency response [41], the low-pass scaling (LPS) α , $0 < \alpha < 1$ and the high-pass scaling (HPS) β , $0 < \beta \leq 1$ are to be selected in order to respect the condition $\alpha + \beta > 1$. This condition ensures perfect reconstruction and avoids redundancy.

The α and β factors are related to the quality factor (Q), redundancy parameter (R) and maximum number of sub-bands (J_{max}) of TQWT, which are defined as [41]: $Q =$

$$\frac{2 - \beta}{\beta} \quad (20)$$

$$R = \frac{\beta}{1 - \alpha} \quad (21)$$

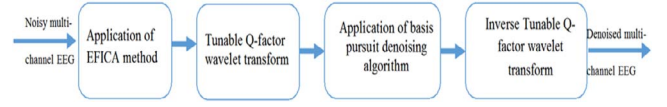


FIGURE 4. General process flow of EFICA-TQWT algorithm.

$$J_{max} = \left(\frac{\log(\beta N / 8)}{\log(1/\alpha)} \right) \quad (22)$$

with N is the length of the analysed signal.

In fact, the procedure of TQWT filtering is the following:

Step 1: Fix the constant bandwidth for each sub-band.

Step 2: Choose the values of TQWT parameters: the Q -factor, the parameter R and the number of decomposition stages J .

Step 3: Calculate the low-pass scaling LPS and the high-pass scaling HPS by using the following equations:

$$LPS = 1 - \frac{(HPS)}{R} \quad (23)$$

$$HPS = \frac{2}{Q + 1} \quad (24)$$

Step 4: Calculate the ratio of center frequency (CF) corresponding to the bandwidth of each sub-band (Eq. 25).

$$CF(j) = (LPS)^j \left[\frac{2 - (HPS)}{4(LPS)} \right] f_s \quad (25)$$

Step 5: Apply the TQWT on the input signal of The TQWT block by adopting the assigned values of Q -factor, R and J . In this case, the TQWT block made the wavelet coefficients of each sub-band except the J^{th} sub-band that is equal to zero.

Step 6: Finally, obtain the sub-band signals by applying the inverse TQWT using the TQWT filter block from the J^{th} sub-band.

3.2.2. Proposed filtering algorithms: hybrid (EFICA-TQWT) algorithm

The EFICA-TQWT algorithm for ocular and muscular artifact removal is based on four main steps (Fig. 4):

(A) The EFICA method is applied to the EEG signal to suppress high-frequency artifacts (muscular artifacts).

(B) To filter the low-frequency artifacts, the radix-2 TQWT [42] is applied to the EEG denoised signal by the EFICA method. The EEG signals corresponding to various channels are decomposed with the same Q , R and J_{max} parameters using the radix-2 TQWT operation. In this work, after a comparative study, the best results were obtained with $Q = 3$, $R = 3$ and $J_{max} = 21$.

(C) The basis pursuit denoising (BPD) algorithm is applied on the out-put EEG signal from EFICA. This approach is based

on the assumption that a signal y is corrupted by additive noise n (Eq. 26):

$$y = x + n \quad (26)$$

In order to estimate the signal x , which has a sparse representation, from the signal y , a sparsity-based method particularly the BPD [43] is implemented. This algorithm using a variation of SALSA [44] reduces the sum of the l1-norm corresponding to the TQWT transform coefficients and the residual energy (Eq.27) [42]:

$$\arg \min_w \| y - TQWT^{-1}(w) \|_2 + \sum_{j=1}^{J+1} \lambda_j \| w_j \|_1 \quad (27)$$

with:

— w_j represents subband j , — $\lambda_j \varepsilon(\lambda_1, \lambda_2, \dots, \lambda_{J+1})$ are regularization parameters,

— $\| \cdot \|_i, i \in \{1, 2\}$, represents respectively the l1 and l2 norm,

— J is the number of filter banks.

The signal x will be estimated as $TQWT^{-1}(w)$. D) The EEG filtering signals are remodeled by applying the inverse TQWT technique (Fig. 3).

3.3. Step 3: the 3D spline interpolation method

Based on the work [21], the 3D spline interpolation method of order three was used in the present paper since it was given the most minimal value of the root mean squared error.

The principle of this algorithm is as follows: it uses the EEG, the position of the real and interpolated electrodes as input and generates in output, by mathematical interpolation, the new values of the electrical activities relative to the virtual electrodes.

Let E_s a set of M less noisy source samples $es_l; l = 1, \dots, M$; where real potential V_{s_l} are measured.

Let ei the point of the noisiest channel, where interpolated potential V_i will be calculated.

Let us denote by (x_i, y_i, z_i) and $(x_{s_l}, y_{s_l}, z_{s_l})$, respectively, the coordinates of ei and es_l points.

The interpolated potential V_i at a point ei is calculated by the 3D spline method according to the following equation (Eq. 28) [21]:

$$V_i = \sum_{l=1}^M P_l h_m(x_i - x_{s_l}, y_i - y_{s_l}, z_i - z_{s_l}) + \sum_{d=0}^{m-1} \sum_{f=0}^d \sum_{g=0}^f q_{dfg} x_i^{d-f} y_i^{f-g} z_i^g \quad (28)$$

where

$$h_m(r, s, t) = (r^2 + s^2 + t^2)^{\frac{2m-3}{2}} \quad (29)$$

In this work, h_m is a polynomial function calculated according to the Cartesian coordinates of the less noisy real electrodes, $(x_{s_l}, y_{s_l}, z_{s_l})$ and those of the noisiest electrode, (x_i, y_i, z_i) with

the order of the 3D spline interpolation equal to three ($m = 3$); where:

$$r^2 = (x_i - x_{s_l})^2 \quad (30)$$

$$s^2 = (y_i - y_{s_l})^2 \quad (31)$$

$$t^2 = (z_i - z_{s_l})^2 \quad (32)$$

P_l and q_{dfg} are obtained by solving the matrix form of Eq. 33 applied to less noisy source points [21]:

$$\begin{pmatrix} H & F \\ F^t & 0 \end{pmatrix} \begin{pmatrix} P \\ Q \end{pmatrix} = \begin{pmatrix} V_s \\ 0 \end{pmatrix} \quad (33)$$

such that:

$$\begin{aligned} -Q &= (q_{000}, q_{100}, q_{110}, q_{111}, \dots, q_{m-1, m-1, m-1})^t, \\ -P &= (P_1, P_2, \dots, P_M)^t, \end{aligned}$$

$$-H = (H_{ij})_{1 \leq i, j \leq M}, \quad (34)$$

with,

$$H_{ij} = h_m(x_i - x_{s_j}, y_i - y_{s_j}, z_i - z_{s_j})$$

— $F =$

$$\begin{pmatrix} 1 & x_{s_1} & y_{s_1} & z_{s_1} & x_{s_1}^2 & x_{s_1} \cdot y_{s_1} & x_{s_1} \cdot z_{s_1} & y_{s_1}^2 & y_{s_1} \cdot z_{s_1} & z_{s_1}^2 & \dots & z_{s_1}^{m-1} \\ \vdots & \dots & \vdots \\ 1 & x_{s_M} & y_{s_M} & z_{s_M} & x_{s_M}^2 & x_{s_M} \cdot y_{s_M} & x_{s_M} \cdot z_{s_M} & y_{s_M}^2 & y_{s_M} \cdot z_{s_M} & z_{s_M}^2 & \dots & z_{s_M}^{m-1} \end{pmatrix} \quad (35)$$

3.4. Step 4: evaluation criteria

In this work, the ocular and muscular removal method was evaluated by calculating two evaluation criteria: MSE and SNR.

Let N the number of EEG signal samples, x_i be the EEG original signal of the sample i , with $1 \leq i \leq N$, — x'_i the EEG filtered signal of sample i , with $1 \leq i \leq N$,

The MSE value is calculated using the Eq. 36 [45]:

$$MSE (\mu V^2) = \frac{\sum_{i=1}^N (x'_i - x_i)^2}{N} \quad (36)$$

The SNR is expressed as (Eq. 37) [45]:

$$SNR \text{ (dB)} = 10 \log_{10} \left[\frac{\sum_{i=1}^N x_i^2}{\sum_{i=1}^N (x'_i - x_i)^2} \right] \quad (37)$$

		Predicted Values	
		Positive	Negative
Actual Values	Positive	TP 39	FN 6
	Negative	FP 0	TN 191

FIGURE 5. Confusion matrix of the SVM.

4. RESULTS AND DISCUSSION

4.1. SVM results

The RBF kernel based SVM classifier system was tested on every recording of the healthy and pathological datasets to extract the most artifactual EEG channel(s). In fact, a training vector was created to train the SVM by taking 354 channels from each of the three used EEG datasets. Then, the proposed SVM algorithm was tested using a testing vector created from the remaining 236 channels.

The performance of the SVM classifier was evaluated using the information extracted from the confusion matrix (Fig. 5), where true positive (TP) and false positive (FP) designate respectively the total number of correctly classified nosiest channels and the amount of actually less noisy EEG channels diagnosed as the nosiest electrodes. Similarly, true negative (TN) and false negative (FN) describe respectively the number of correctly classified less noisy channels, and the nosiest electrodes incorrectly classified as the least artifactual EEG channels.

The receiver operating characteristics parameters such as accuracy, specificity and sensitivity were calculated for the used SVM model. Equations 38, 39 and 40 were used to calculate these evaluation parameters during the testing phase [46]:

$$accuracy (\%) = \frac{100 \times (TN + TP)}{TN + TP + FN + FP} \quad (38)$$

$$Sensitivity (\%) = \frac{100 \times TP}{TP + FN} \quad (39)$$

$$Specificity (\%) = \frac{100 \times TN}{TN + FP} \quad (40)$$

In order to justify the choice of a good classifier based on the three kernels of SVM (linear, polynomial and RBF), the validation metrics (accuracy, sensitivity and specificity) were calculated by considering the test channels of the three datasets used (Table 2).

TABLE 2. Comparative table of Kernel SVM performance.

Kernel	Accuracy (%)	Sensitivity (%)	Specificity (%)
Linear	88.48	71.05	95.82
RBF	97.45	86.66	100
Second degree polynomial	90.02	72.9	98.73
Third degree polynomial	93.74	75.2	100

Table 2 shows that using the RBF kernel provides the best classification performance compared to the linear and both second and third degree polynomial kernels, since it produces an accuracy of 97.45%, a sensitivity of 86.66% and a 100% specificity in classifying all testing channels. In fact, to calculate the accuracy, sensitivity and specificity, the RBF SVM has been trained by using several values of C and γ parameters. In this work, these parameters are selected since they give the highest accuracy. The best results are found by setting C to 1 and γ to 0.4 (Table 3).

So according to the results found in Table 2 and 3, the RBF SVM classifier (with C = 1 and $\gamma = 0.4$) is adopted in order to have an efficient classification. In this case, Table 4 presents a comparison between the results found by the SVM classifier and the classification of an expert in physiology. The results show that 6 channels have been designated as false negative channels and 39 channels have been classified as true positive channels. The false negative and the true positive channels are defined respectively in the output of SVM classifier as status '0' and '1'. Each signal corresponding to an identified noisy channel will be eliminated in order to apply the filtering process to other least artifactual EEG channels for each subject.

In this case, the confusion matrix that is obtained for the test channels (236 channels) is defined in the Fig. 5.

4.2. Filtering results

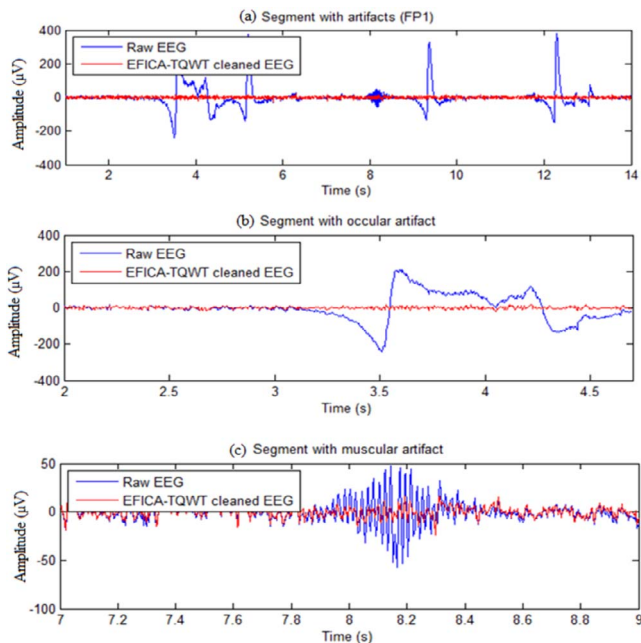
4.2.1. Analysis I: comparison without interpolation

Before testing the interpolation effect on EEG signal filtering, this work will test the performance of the developed EFICA-TQWT hybrid method on the EEG signal. This technique is applied to the real FP1 EEG signal corresponding to healthy subject 1. This real portion of FP1-EEG signal is characterized by the presence of ocular and muscular artifacts (Fig. 6).

To distinguish the filtering method performance proposed for eliminating ocular and muscular artifacts, while preserving useful neural information, a separation of the raw EEG data into three regions: 'EEG with ocular artifacts', 'EEG with muscular artifacts' and 'EEG without ocular and muscular artifacts' was performed. For example, Fig. 6 shows the effect of filtering by the EFICA-TQWT method on an FP1 electrode recording with a duration of 14 s characterized by the presence of ocular and muscular noises (according to an expert). The major ocular

TABLE 3. Evaluation of RBF kernel SVM classifier performances by varying γ and C .

Performances	Gamma variation	$0.01 \leq C \leq 0.56$	$0.56 < C \leq 0.9$	$C \geq 1$
Accuracy (%)	$\gamma = 0.1$	80.09	85.67	93.85
	$\gamma = 0.4$	83.15	87.95	97.45
	$\gamma = 1$	67.02	71.29	83.71
Sensitivity (%)	$\gamma = 0.1$	75.37	77.43	82.9
	$\gamma = 0.4$	76.93	83.54	86.66
	$\gamma = 1$	70.18	76.07	76.46
Specificity (%)	$\gamma = 0.1$	70.23	80.58	88.51
	$\gamma = 0.4$	76.35	82.73	100
	$\gamma = 1$	68.97%	73.22%	90%

**FIGURE 6.** Filtering noisy EEG portion of FP1 channel with (a) both ocular and muscular, (b) ocular and (c) muscular artifacts.

artifact appears at the third second. The eye-blinking artifact appears in EEG as big pulses well localized in time. However, the muscular artifact emerges at second 7.9 of EEG recording.

For Fig. 6, a careful observation shows that EFICA-TQWT exquisitely produced cleaner processed signals in both cases of ocular and muscular artifacts. In addition, this method shows a great efficiency and competence for preserving neuronal information in the non-artifact region.

To effectively show the performance of the EFICA-TQWT technique, Table 5 gives the found SNR and MSE corresponding to 1-minute recording of noisy single FP1 channel of healthy subject 1 filtering with the hybrid EFICA-TQWT method. The results show that this method offers a high SNR rate with a low MSE value for both OA and MA

categories. The SNR and MSE in the case of MA are more important since this type of artifact occupies a larger amount in this FP1 EEG signal.

To better demonstrate the effectiveness of this hybrid method, the EFICA, classical fast-ICA, TQWT and DWT methods were applied on the three datasets used in this work in order to perform a comparative study between these methods and the EFICA-TQWT. Table 6 shows the MSE and SNR means of these methods applied on the different EEG signals from the three datasets.

According to Table 6, the five methods (Fast-ICA, DWT, TQWT, EFICA and EFICA-TQWT) show a higher efficiency in filtering the muscular and ocular artifacts, more particularly in the case of healthy subjects (datasets 1 and 3). Indeed, the SNR in all cases of healthy subjects is larger than that in epileptic patients (dataset 2). This means that healthy EEG signals are more infected by these types of physiological noise (ocular and muscular).

Moreover, Table 6 shows that the hybrid EFICA-TQWT algorithm improves the quality of ocular and muscular artifact removal by comparing it to other methods. More precisely, the EFICA-TQWT offered good results by giving the lowest MSE average ($0.361 \mu V^2$) and highest SNR mean (17.63 dB). In fact, this proposed hybrid method (EFICA-TQWT) is slightly effective in terms of removing noise, especially in the case of healthy dataset 3 by offering the significant value of SNR (36.15 dB) compared more particularly to epileptic dataset 2. This result asserts that the EFICA-TQWT method can distinguish ocular and muscular artifacts from other types of artifacts or epileptic waves.

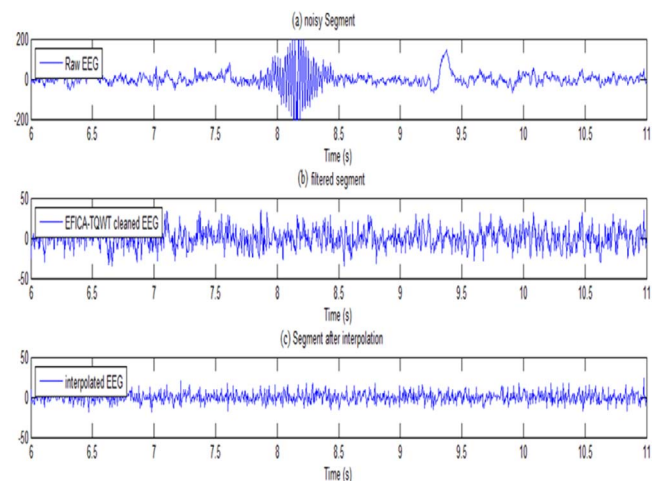
However, the DWT and TQWT methods show the worst results. This can be explained by the fact that these methods are characterized by the removal of artifacts of low frequencies (ocular). Moreover, although fast-ICA and EFICA give better results than the DWT and TQWT method, they remain less efficient than the hybrid EFICA-TQWT filter since they remove only high frequency artifacts (muscular). To remedy this problem, the combination of the EFICA method with the TQWT will be a primordial necessity. This combination

TABLE 4. SVM classifier results.

Dataset	Subject	Noisiest channel (according to the expert)	SVM result	
Dataset 1	Subject 1	FP1	TP	
		CZ	TP	
	Subject 2	T3	TP	
Dataset 2	Subject 3	F7	TP	
		F3	FN	
	A0005	P3	TP	
	A0018	C3	TP	
	A0019	P4	FN	
	A0022	F4	TP	
	A0024	C1	TP	
Dataset 3	A0032	F4	FN	
	2272	F8	TP	
		T3	TP	
		2508	F3	TP
			F4	TP
		2705	T3	TP
		5221	F8	TP
			T4	TP
	5394	C4	TP	
		T3	TP	
		T6	TP	
	5398	F7	TP	
		F8	TP	
	5457	T3	TP	
		F7	TP	
	5655	T3	TP	
		F7	TP	
	5851	F8	TP	
		F7	TP	
	5921	F8	TP	
		T3	TP	
	6061	T3	TP	
	6076	F8	TP	
6088	T4	TP		
6201	T3	FN		
6215	FP2	FN		
6238	F7	TP		
6317	FP1	FN		
6322	FP2	TP		
6422	C4	TP		
7020	F8	TP		
	T3	TP		
	7481	FP1	TP	
	7647	FP2	TP	
	7679	F7	TP	

TABLE 5. The MSE and SNR of filtering FP1 EEG signal of healthy subject 1 by EFICA-TQWT method.

Real FP1 EEG	SNR (dB)	MSE (μV^2)
Total signal (60s)	12.05	0.74
Portion with ocular artifact (3 s to 4.7 s)	13.84	0.54
Portion with muscular artifact (7.9 s to 8.5 s)	17.32	0.67

**FIGURE 7.** T3 channel EEG portion of the healthy subject 2 (a) with artifacts, (b) filtered by EFICA-TQWT without interpolation and (c) filtered by EFICA-TQWT with interpolation.

offers a more effective improvement to ocular and muscular artifact removal with the ability to provide a filtered EEG signal without information loss.

4.2.2. Analysis II: comparison with interpolation

According to the previous subsection, the EFICA-TQWT filtering method gives the best results. For this, this method will be adopted in this section to study the effect of 3D spline interpolation on the filtering efficiency of EEG signals.

Let us take the example of the healthy subject 2 from dataset 1. Figure 7 presents the denoised T3-channel signals (Table 4) during a 6 s up to 11 s period obtained when the hybrid proposed filtering algorithm EFICA-TQWT, with and without interpolation, is used to remove artifacts in the real EEG signal. Based on visual examination, the muscular and ocular artifacts contaminating the T3-channel are presented respectively from 7.9 s to 8.5 s and 9.4 s to 9.5 s. These muscular and ocular artifacts are removed by the EFICA-TQWT method using the interpolation technique (Fig. 7 (c)).

Figure 7 shows a higher performance of filtering in the case of EFICA-TQWT with T3 interpolation. In fact, muscular artifact removal based on EFICA-TQWT without interpolation reduces the noise level found in the EEG signal. However,

TABLE 6. Comparison of MSE and SNR for the EEG datasets.

Criterion method	Dataset 1		Dataset 2		Dataset 3		Average	
	SNR (dB)	MSE (μV^2)	SNR (dB)	MSE (μV^2)	SNR (dB)	MSE (μV^2)	SNR (dB)	MSE (μV^2)
Fast-ICA	7.987	1.129	2.709	0.795	22.26	0.798	10.98	0.907
DWT	5.265	1.574	1.857	1.168	16.39	1.083	7.83	1.275
EFICA	9.758	0.917	3.267	0.585	28.49	0.716	13.83	0.739
TQWT	6.641	1.209	2.258	0.831	19.94	0.952	9.613	0.997
EFICA-TQWT	11.948	0.468	4.82	0.208	36.15	0.409	17.63	0.361

TABLE 7. Comparison of MSE and SNR of EEG signal corresponding to T3 electrode for the healthy subject 2.

Method	Without interpolation		With T3 interpolation	
	SNR(dB)	MSE(μV^2)	SNR(dB)	MSE(μV^2)
EFICA-TQWT	18.698	0.482	25.718	0.22

with a large amount of MA characterized by great amplitude (between $-200 \mu\text{V}$ and $200 \mu\text{V}$) and wide impulses, it is insufficient to have a raw EEG signal with only useful neural information. The appeal of the 3D spline interpolation method offers a better result with total elimination of muscular and ocular artifacts.

Table 7 compares the performance criteria achieved by applying the proposed filtering method (EFICA-TQWT) only on 1-minute EEG signal of T3 channel in two cases: filtering with and without using T3 interpolation.

According to Table 7, the filtering method gives better results when using the 3D spline interpolation technique by giving the highest SNR and the smallest MSE.

Moreover, the proposed hybrid system performance not only applies to the EEG recordings with a single noisy channel, but greater efficiency has been shown for noisy multi-channel signals. For example, Fig. 8 presents a 14-second EEG recording of a patient from dataset 3 characterized by the presence of intense muscular and ocular artifacts, more particularly in three channels (T3, C4 and T6). Likewise, the EFICA-TQWT filtering method with and without interpolation is applied to this EEG recording (Fig. 8).

Figure 8 shows that both EFICA-TQWT with and without interpolation allow very effective filtering of less noisy channels by muscular and ocular artifacts. However, EFICA-TQWT seems less efficient in the case of channel filtering with intense artifacts. The solution to improve filtering must be provided by the hybrid method with the 3D spline. In fact, the 3D spline technique is a global interpolation method that allows a proper estimation of the channels to be interpolated, even if they are deputies, with minimal error [21]. This 3D spline feature makes it possible to build well filtered EEG signals from the other real filtered channels, even if the SVM classification system shows several positive channels (very noisy).

Table 8 gives the different SNR and MSE measured by the two methods (with and without interpolation) over a 1-minute period.

Table 9 presents the average performances according to MSE and SNR metrics of studied filtering method EFICA-TQWT with 3D spline interpolation for the multi-channel EEG of each healthy (dataset 1 and 3) and pathological (dataset 2) subjects.

Table 9 shows that the EFICA-TQWT with 3D spline allows high performance in filtering EEG signals, especially for signals highly noisy by ocular and muscular artifacts (dataset 3). However, the SNR of dataset 2 corresponding to EFICA-TQWT with interpolation (6.123 dB) does not provide much improvement over that of EFICA-TQWT without 3D spline (4.82 dB). This is explained by the presence of weak artifacts in this dataset. Nevertheless, the EFICA-TQWT with interpolation is highly efficient in terms of SNR (24.124 dB) and MSE ($0.131 \mu\text{V}^2$) averages compared to that without interpolation (SNR = 17.63 dB and MSE = $0.361 \mu\text{V}^2$).

These results are very satisfactory compared to other works. In fact, different datasets were used in the literature to validate the filtering methods. For example, the authors in [47] utilized EEG signals recorded using 32 channels from healthy and disabled subjects. In this work, the study was carried out to compare three methods (translation invariant wavelet transform: TI-WT, fast-ICA and radical algorithms) used in artifact removal. The TI-WT gave the best results with an SNR nearer to zero and a smaller MSE (compared to other methods) of $1.00\text{e}+03$. In addition, the authors in [48] found that the proposed algorithm based on the multi-channel Wiener filter for eye blink artifact removal gave a mean SNR around 12 dB. In [49], the authors utilized the ICA as a BSS technique for removing mobility artifacts. The ICA method gave an SNR almost equal to 11 dB.

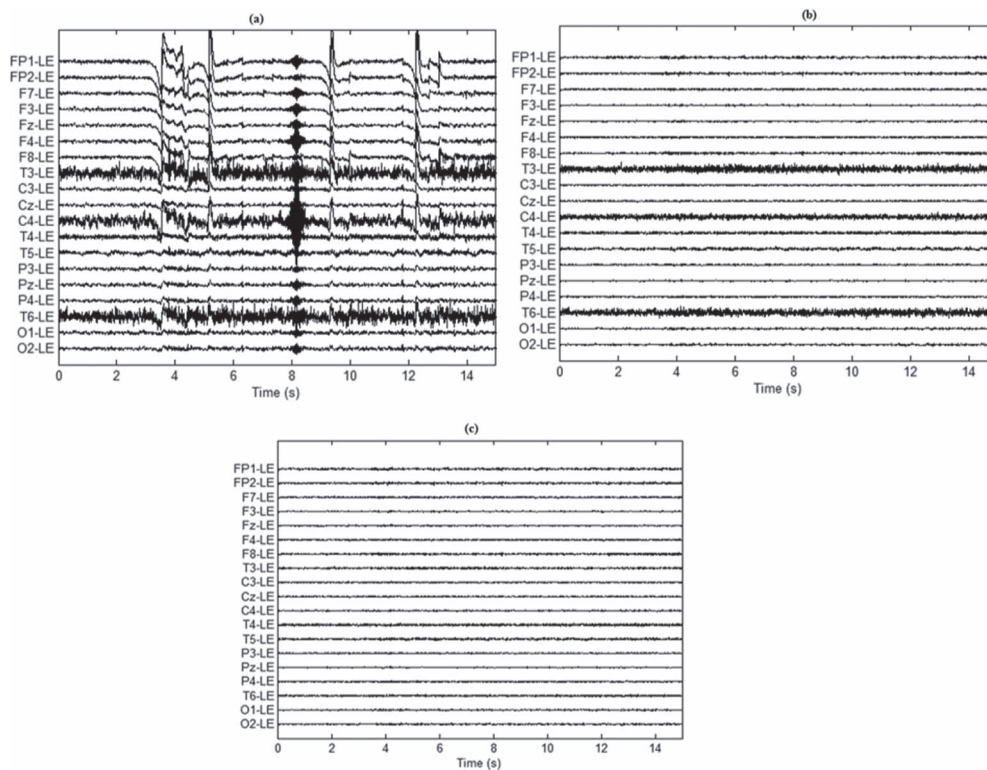


FIGURE 8. Multi-channel EEG signals of healthy subject from dataset 3: (a) with artifacts, (b) filtered by EFICA-TQWT, filtered by EFICA-TQWT with spline 3D.

TABLE 8. Comparison of MSE and SNR of EEG signal corresponding to a healthy subject from dataset 3.

Channel	EFICA-TQWT without interpolation		EFICA-TQWT with T3 interpolation	
	SNR (dB)	MSE (μV^2)	SNR (dB)	MSE (μV^2)
T3	30.38	0.582	34.49	0.399
C4	32.49	0.632	37.78	0.581
T6	26.87	0.593	39.53	0.460
Total of 19 channel over a 1-minute period	28.39	0.573	31.57	0.377

TABLE 9. Comparison of MSE and SNR of EFICA-TQWT with 3D spline for the EEG datasets.

Criterion method	Dataset 1		Dataset 2		Dataset 3		Average	
	SNR (dB)	MSE (μV^2)	SNR (dB)	MSE (μV^2)	SNR (dB)	MSE (μV^2)	SNR (dB)	MSE (μV^2)
EFICA-TQWT with 3D spline	17.60	0.168	6.123	0.091	48.65	0.135	24.124	0.131

In addition, in [50] several pre-processing filters were tested on EEG data, such as self-filter, Kalman filter, recurrent quantum neural network filter, moving average filter, modified self-filter, Savitzky Golay filter and Weiner filter. A study was conducted to find the best pre-processing technique for cleaning

EEG signals. From the results obtained, it was concluded that the self-filter showed the best results when compared to other filtering techniques. In fact, the self-filter exhibited a maximum SNR value equal to 24.83 dB and an MSE equal to $0.404 \mu V^2$ for random noise signals.

TABLE 10. Execution time of different filtering process algorithms on CPU and GPU.

Algorithm	CPU execution time in seconds	GPU execution time in seconds	Optimization rate%
SVM classification	0.389	0.207	46.78
EFICA-TQWT (18 channel filtering for 1 minute)	15.705	8.352	46.81
3D Spline (interpolation of a single channel over 1 minute)	8.694	4.46	48.70
Total	24.788	13.019	47.47

4.3. Computational times of EFICA-TQWT with interpolation

In addition to providing a hybrid EEG signal filtering system based on interpolation, the current work is also aimed at optimizing the calculation times of this system in order to increase the efficiency of the proposed algorithm in terms of execution time and meet the requirement of real-time processing. In particular, the proposed hybrid EEG filtering method is implemented independently in a sequential MATLAB version for the CPU and a MATLAB/compute unified device architecture (CUDA) version for the GPU. The choice of GPU is justified by the presence of several thousand threads on GPU. These threads make this graphical processing look similar to a super calculator rather than a multi-core CPU, which allows only a few threads to be treated simultaneously.

In fact, all calculations realized in this work were performed on an Intel (R) Core™i7-5500U, fifth generation CPU 2.4 GHz with RAM 8Go and NVIDIA Ge Force 820 M. The GPU used is of Fermi architecture with 96 CUDA cores, 2GB DDR3 and 1800 MHz device memory, where the MATLAB version is R2017a, the Visual Studio version used is 2015 prof with NVIDIA CUDA Toolkit 8.0.

In this paper, both C++ and MATLAB were used. These two languages can be used alone but using both at the same time gives more benefits. MATLAB is linked with CUDA C++ in two cases; either when MATLAB is not able to run an existing piece of code on GPU, or when the highly optimized libraries of CUDA is used. The acceleration process consists in using the CUDA with .mex file. An input/output analysis and memory allowance are achieved after creating a .mex file. In this case, the parallel computation represented in the function 'loop for' is realized in the GPU and the sequential computation is executed in the CPU. In this work, the parallelism between the different threads in the same block was adopted by using the shared memory. This memory allows the reduction of memory access latency and greatly improves the GPU algorithm performance. The results will be transmitted to the MATLAB and the memory will be free.

The execution time of the proposed filtering method available in CPU is compared with the processing time on GPU. Indeed, the calculated time corresponds to three phases: the first phase consists in classifying the channels into noisier and less

noisy channels. The second step filters the EEG signals from 18 channels. Interpolation of the noisiest EEG channel by the 3D spline method on 1-minute samples is the last phase.

To justify the performance of GPU and the parallel computing, the optimization rate, which measures the obtained gain time of a parallel algorithm compared to a corresponding sequential algorithm, is calculated as (Eq. 41):

$$\text{Optimization rate (\%)} = 100 \times \left(1 - \frac{\text{Parallel execution time}}{\text{Sequential execution time}} \right) \quad (41)$$

Table 10 shows the optimization rate of the proposed hybrid filtering system. The results show that the execution time generated by CPU is significantly more important than the GPU. The optimization rate mean reaches 47.47% when shared memory is utilized and MATLAB is used with c-mex and CUDA.

5. CONCLUSION

In conclusion, the aim of the present paper is to provide hybrid ocular and muscular artifact removal for multi-channel EEG of healthy and pathological subjects. First, an RBF kernel-based SVM classifier was used to extract the noisiest channel(s) from the EEG multi-channel of each subject. Secondly, the hybrid EFICA-TQWT method was applied to the remaining less noisy channels of the EEG recording. Thirdly, the eliminated signal(s) was (were) reconstructed from the other filtered channels by using the 3D spline interpolation technique. The performance of the proposed hybrid method was evaluated by the calculation of the MSE and SNR criteria. The results showed that the hybrid EFICA-TQWT method with 3D spline interpolation gave the best results compared to the EFICA-TQWT algorithm without interpolation. Finally, a GPU implementation of the proposed hybrid filtering system with 3D spline was performed using CUDA and C++ with .mex file. The results showed that the GPU implementation gave an optimization rate of 47.47% compared to a CPU implementation.

5. DATA AVAILABILITY

The dataset 1 underlying this article will be shared on reasonable request to the corresponding author.

The dataset 2 underlying this article is available in EEG database at <https://doi.org/10.1177/1550059413500960>.

The dataset 3 underlying this article is available in 01_tcp_ar, at https://www.isip.piconepress.com/projects/tuh_eeg/downloads/. The dataset was derived from the Temple University Medical Center at https://www.isip.piconepress.com/projects/tuh_eeg/html/downloads.shtml.

Acknowledgements

The authors are grateful to Dr Mohamed Ali Saafi, Associate Professor of the Physiology Laboratory at the Medicine Faculty of Monastir and at the Department of Functional Investigations of the Nervous System (Sahloul University Hospital, Sousse-Tunisia) for his invaluable discussion. Dr Mohamed Ali Saafi provided this work, the multi-channel EEG signals of the three healthy subjects collected at Sahloul Hospital, Sousse-Tunisia. He contributed to this research work by selecting the EEG recordings of datasets 2 and 3, containing the muscular and ocular artifacts. He classified the noisiest electrodes for each EEG recording in order to compare the results found by the SVM classification with the expert classification.

Conflict of interest

The authors declare that the research was conducted in the absence of any business or financial relationship that could be interpreted as a potential conflict of interest.

REFERENCES

- [1] Ahammad, N., Fathima, T. and Joseph, P. (2014) Detection of epileptic seizure event and onset using EEG. *BioMed Res. Int.*, 7, 1–7.
- [2] Sairamya, N.J., George, S.T., Ponraj, D.N. and Subathra, M.S.P. (2018) Detection of epileptic EEG signal using improved local pattern transformation methods. *Circuits Syst. Signal Process.*, 37, 5554–5575.
- [3] Sanei, S. and Chambers, J.A. (2007) *EEG Signal Processing*. John Wiley & Sons Ltd., Chichester.
- [4] Teplan, M. (2002) Fundamentals of EEG measurement. *Meas. Sci. Rev.*, 2, 1–11.
- [5] Mateo-Sotos, J., Torres, A.M., Sánchez-Morla, E.V. and Santos, J.L. (2016) An adaptive radial basis function neural network filter for noise reduction in biomedical recordings. *Circuits Syst. Signal Process.*, 35, 4463–4485.
- [6] Winkler, I., Haufe, S. and Tangermann, M. (2011) Automatic classification of artifactual ICA-components for artifact removal in EEG signals. *Behav. Brain Funct.*, 7, 30.
- [7] Iwasaki, M., Kellinghaus, C., Alexopoulos, A.V., Burgess, R.C., Kumar, A.N., Han, Y.H. and Leigh, R.J. (2005) Effects of eyelid closure, blinks, and eye movements on the electroencephalogram. *Clin. Neurophysiol.*, 116, 878–885.
- [8] Goncharova, I.I., McFarland, D.J., Vaughan, T.M. and Wolpaw, J.R. (2003) EMG contamination of EEG: spectral and topographical characteristics. *Clin. Neurophysiol.*, 114, 1580–1593.
- [9] Helal, A.E.M., Seddik, A.F. and Hussein, A.A.F. (2017) A hybrid approach for artifacts removal from EEG recordings. *Int. J. Comput. Appl.*, 168, 10–19.
- [10] Tibdewal, M.N., Fate, R.R., Mahadevappa, M., Ray, A.K. and Malokar, M. (2017) Classification of artifactual EEG signal and detection of multiple eye movement artifact zones using novel time-amplitude algorithm. *Signal Image Video Process.*, 11, 333–340.
- [11] Halder, S., Bensch, M., Mellinger, J., Bogdan, M., Kübler, A., Birbaumer, N. and Rosenstiel, W. (2007) Online artifact removal for brain-computer interfaces using support vector machines and blind source separation. *Comput. Intell. Neurosci.*, 7, 1–10.
- [12] Hung, C.I., Lee, P.L., Wu, Y.T., Chen, L.F., Yeh, T.C. and Hsieh, J.C. (2005) Recognition of motor imagery electroencephalography using independent component analysis and machine classifiers. *Ann. Biomed. Eng.*, 33, 1053–1070.
- [13] Wallstrom, G.L., Kass, R.E., Miller, A., Cohn, J.F. and Fox, N.A. (2004) Automatic correction of ocular artifacts in the EEG: a comparison of regression-based and component-based methods. *Int. J. Psychophysiol.*, 53, 105–119.
- [14] Srinivasulu, A. and Reddy, M.S. (2012) Artifacts removing from EEG signals by ICA algorithms. *IOSR J. Electr. Electron. Eng. (IOSRJEEE)*, 2, 11–16.
- [15] Kumar, P.S., Arumuganathan, R., Sivakumar, K. and Vimal, C. (2008) Removal of ocular artifacts in the EEG through wavelet transform without using an EOG reference channel. *Int. J. Open Problems Compt. Math.*, 1, 188–200.
- [16] Krishnaveni, V., Jayaraman, S., Anitha, L. and Ramadoss, K. (2006) Removal of ocular artifacts from EEG using adaptive thresholding of wavelet coefficients. *J. Neural Eng.*, 3, 338–346.
- [17] Yong, X., Fatourech, M., Ward, R.K. and Birch, G.E. (2012) Automatic artefact removal in a self-paced hybrid brain-computer interface system. *J. Neuroeng. Rehabil.*, 9, 50.
- [18] Sabarigiri, B. and Suganyadevi, D. (2014) A hybrid pre-processing techniques for artifacts removal to improve the performance of electroencephalogram (EEG) features extraction. *Int. J. Innov. Res. Sci. Eng. Technol.*, 3, 2087–2092.
- [19] Garg, H.K. and Kohli, A.K. (2017) Excision of ocular artifacts from EEG using NVFF-RLS adaptive algorithm. *Circuits Syst. Signal Process.*, 36, 404–419.
- [20] Huang, X. and Zeng, H. (2012) Efficient variant of FastICA algorithm for speech features extraction. *Lect. Notes Electr. Eng.*, 113, 929–935.
- [21] Nouira, I., Abdallah, A.B. and Bedoui, M.H. (2016) Three-dimensional interpolation methods to spatiotemporal EEG mapping during various behavioral states. *Signal Image Video Process.*, 10, 943–949.
- [22] Selvaraj, T.G., Ramasamy, B., Jeyaraj, S.J. and Suvisheshamuthu, E.S. (2014) EEG database of seizure disorders for experts and application developers. *Clin. EEG Neurosci.*, 45, 304–309. doi: [10.1177/1550059413500960](https://doi.org/10.1177/1550059413500960).
- [23] Richhariya, B. and Tanveer, M. (2018) EEG signal classification using universum support vector machine. *Exp. Syst. Appl.*, 106, 169–182.

- [24] Zhang, Y., Dong, Z., Liu, A., Wang, S., Ji, G., Zhang, Z. and Yang, J. (2015) Magnetic resonance brain image classification via stationary wavelet transform and generalized eigenvalue proximal support vector machine. *J. Med. Imag. Health Inform.*, 5, 1395–1403.
- [25] Zhang, Y., Dong, Z., Wang, S., Ji, G. and Yang, J. (2015) Pre-clinical diagnosis of magnetic resonance (MR) brain images via discrete wavelet packet transform with Tsallis entropy and generalized eigenvalue proximal support vector machine (GEP-SVM). *Entropy*, 17, 1795–1813.
- [26] Wang, S., Lu, S., Dong, Z., Yang, J., Yang, M. and Zhang, Y. (2016) Dual-tree complex wavelet transform and twin support vector machine for pathological brain detection. *Appl. Sci.*, 6, 169.
- [27] Gupta, S. and Mohan Singh, M. (2017) Diagnosing epilepsy using EEG signals and classification of EEG signals using SVM. *Int. Res. J. Eng. Technol.*, 4, 2914–2916.
- [28] Nanthini, B.S. and Santhi, B. (2014) Seizure detection using SVM classifier on EEG signal. *J. Appl. Sci.*, 14, 1658–1661.
- [29] Vipani, R., Hore, S., Basak, S. and Dutta, S. (2018) Hilbert transform and RBF-kernel based support vector machine synergy for automatic classification of EEG signals. *Int. J. Latest Trends Eng. Technol.*, 9, 22–28.
- [30] Bousseta, R., Tayeb, S., El Ouakouak, I., Gharbi, M., Regragui, F. and Himmi, M.M. (2018) EEG efficient classification of imagined right and left hand movement using RBF kernel SVM and the joint CWT_PCA. *AI Soc.*, 33, 621–629.
- [31] Awad, M. and Khanna, R. (2015) Support vector machines for classification. In *Efficient Learning Machines*. Apress, Berkeley, California.
- [32] Subasi, A. and Gursoy, M.I. (2010) EEG signal classification using PCA, ICA, LDA and support vector machines. *Exp. Syst. Appl.*, 37, 8659–8666.
- [33] Temko, A., Thomas, E., Marnane, W., Lightbody, G. and Boylan, G. (2011) EEG-based neonatal seizure detection with support vector machines. *Clin. Neurophysiol.*, 122, 464–473.
- [34] Wang, L., Li, J., Zhu, R., Xu, L., He, Y., Zhang, R. and Rao, S. (2011) A novel stepwise support vector machine (SVM) method based on optimal feature combination for predicting miRNA precursors. *African J. Biotechnol.*, 10, 16720–16731.
- [35] Koldovsky, Z., Tichavsky, P. and Oja, E. (2006) Efficient variant of algorithm FastICA for independent component analysis attaining the Cramér–Rao lower bound. *IEEE Trans. Neural Netw.*, 17, 1265–1277.
- [36] Hyvarinen, A. (1999) Fast and robust fixed-point algorithms for independent component analysis. *IEEE Trans. Neural Netw.*, 10, 626–634.
- [37] Yuan, L., Zhou, Z., Yuan, Y. and Wu, S. (2018) An improved FastICA method for fetal ECG extraction. *Comput. Math. Methods Med.* doi: 10.1155/2018/7061456.
- [38] Bhattacharyya, A., Pachori, R.B., Upadhyay, A. and Acharya, U.R. (2017) Tunable-Q wavelet transform based multiscale entropy measure for automated classification of epileptic EEG signals. *Appl. Sci.*, 7, 385.
- [39] Bhattacharyya, A., Pachori, R.B. and Acharya, U.R. (2017) Tunable-Q wavelet transform based multivariate sub-band fuzzy entropy with application to focal EEG signal analysis. *Entropy*, 19, 99.
- [40] Selesnick, I.W. (2011) Wavelet transform with tunable Q-factor. *IEEE Trans. Signal Process.*, 59, 3560–3575.
- [41] Patidar, S., Pachori, R.B., Upadhyay, A. and Acharya, U.R. (2017) An integrated alcoholic index using tunable-Q wavelet transform based features extracted from EEG signals for diagnosis of alcoholism. *Appl. Soft Comput.*, 50, 71–78.
- [42] Selesnick, I. W. (2011) *TQWT toolbox guide*. Electrical and Computer Engineering, Polytechnic Institute of New York University, USA. <http://eeweb.poly.edu/iselesni/TQWT/index.html>.
- [43] Chen, S.S., Donoho, D.L. and Saunders, M.A. (2001) Atomic decomposition by basis pursuit. *SIAM Rev.*, 43, 129–159.
- [44] Afonso, M.V., Bioucas-Dias, J.M. and Figueiredo, M.A. (2010) Fast image recovery using variable splitting and constrained optimization. *IEEE Trans. Image Process.*, 19, 2345–2356.
- [45] Ahirwal, M.K., Kumar, A. and Singh, G.K. (2013) Descendent adaptive noise cancellers to improve SNR of contaminated EEG with gradient-based and evolutionary approach. *Int. J. Biomed. Eng. Technol.*, 13, 49–68.
- [46] Drotár, P., Mekyska, J., Rektorová, I., Masarová, L., Smékal, Z. and Faundez-Zanuy, M. (2014) Decision support framework for Parkinson’s disease based on novel handwriting markers. *IEEE Trans. Neural Syst. Rehabil. Eng.*, 23, 508–516.
- [47] Walters-Williams, J. and Li, Y. (2011) Using invariant translation to denoise electroencephalogram signals. *Am. J. Appl. Sci.*, 8, 1122–1130.
- [48] Somers, B., Francart, T. and Bertrand, A. (2018) A generic EEG artifact removal algorithm based on the multi-channel wiener filter. *J. Neural Eng.*, 15, 036007.
- [49] Islam, M.S., El-Hajj, A.M., Alawieh, H., Dawy, Z., Abbas, N. and El-Imad, J. (2020) EEG mobility artifact removal for ambulatory epileptic seizure prediction applications. *Biomed. Signal Process. Contr.*, 55, 101638.
- [50] Gupta, G.S., Bhatnagar, M., Kumar, S. and Sinha, R.K. (2020) A comparative study of application of different non-conventional filters on electroencephalogram. *Biomed. Res.*, 31, 13–21.